

Accepted Manuscript

Computer simulating a clinical trial of a load-bearing implant:
example of an intramedullary prosthesis

P.J. Prendergast, P.E. Galibarov, C. Lowrey, A.B. Lennon

PII: S1751-6161(11)00153-6
DOI: 10.1016/j.jmbbm.2011.06.005
Reference: JMBBM 381

To appear in: *Journal of the Mechanical Behavior of
Biomedical Materials*

Received date: 11 January 2011
Revised date: 8 June 2011
Accepted date: 9 June 2011



Please cite this article as: Prendergast, P.J., Galibarov, P.E., Lowrey, C., Lennon, A.B.,
Computer simulating a clinical trial of a load-bearing implant: example of an intramedullary
prosthesis. *Journal of the Mechanical Behavior of Biomedical Materials* (2011),
doi:10.1016/j.jmbbm.2011.06.005

This is a PDF file of an unedited manuscript that has been accepted for publication. As a service to our customers we are providing this early version of the manuscript. The manuscript will undergo copyediting, typesetting, and review of the resulting proof before it is published in its final form. Please note that during the production process errors may be discovered which could affect the content, and all legal disclaimers that apply to the journal pertain.

1

2 **Computer simulating a clinical trial of a load-bearing**
3 **implant: example of an intramedullary prosthesis.**

4

5 **P.J. Prendergast, P.E. Galibarov, C. Lowrey & A.B. Lennon**

6

7

8 Trinity Centre for Bioengineering

9 School of Engineering

10 Trinity College

11 Dublin 2

12 Ireland

13

14 Tel.: +353 1 8961383

15 Fax: +353 1 6795554

16

17 Email.: pprender@tcd.ie

18

19

20 Submitted to *Journal of the Mechanical Behaviour of Biomedical Materials*

21

22 First submitted: January 2011

23 Revision Submitted, May 2011

24

1

2 **Abstract**

3 Computational modelling is becoming ever more important for obtaining regulatory
4 approval for new medical devices. An accepted approach is to infer performance in
5 a population from an analysis conducted in an idealized or 'average' patient; we
6 present here a method for predicting the performance of an orthopaedic implant
7 when released into a population - effectively simulating a clinical trial. Specifically
8 we hypothesise an analysis based on a method for predicting the performance in a
9 population will lead to different conclusions than an analysis based on an idealised
10 or 'average' patient. To test this hypothesis we use a finite element model of an
11 intramedullary implant in a bone whose size and remodelling activity is different
12 for each individual in the population. We compare the performance of a low
13 Young's modulus implant ($E = 20$ GPa) to one with a higher Young's modulus (200
14 GPa). Cyclic loading is applied and failure is assumed when the migration of the
15 implant relative to the bone exceeds a threshold magnitude. The analysis in an
16 idealized of 'average' patient predicts that the lower modulus device survives
17 longer whereas the analysis simulating a clinical trial predicts no statistically-
18 significant tendency ($p=0.77$) for the low modulus device to perform better. It is
19 concluded that population-based simulations of implant performance – simulating
20 a clinical trial – presents a very valuable opportunity for more realistic
21 computational pre-clinical testing of medical devices.

22 **Keywords**

23 Simulated clinical trials, intramedullary fixation, stochastic model, finite element
24 analysis, mechanobiology

1 1 Introduction

2 Computational analysis of biomechanical implants has been performed ever since
3 finite element modelling emerged as a practical tool for analysing complex shapes.
4 In the early days the clinical utility was limited because of the lack of
5 computational power; often simple two-dimensional geometries were used
6 (Huiskes and Chao, 1983; Prendergast, 1997). As computational power increased
7 models did improve as patient-specific geometries derived from medical images
8 could be modelled more easily. With patient-specific geometric modelling,
9 limitations of loading and material properties could be addressed; daily loading
10 datasets were developed (Bergmann et al., 2001; Heller et al., 2005) and models
11 incorporating more advanced patient-specific material properties were advanced
12 (see for example Helgason et al., 2008). Current technologies now allow for
13 accurate modelling, corroborated against experimental or other data for many
14 types of medical device, e.g. for orthopaedic implants (Verdonschot and Huiskes,
15 1997; Taylor and Barrett, 2003; Stolk et al., 2007; Lennon et al., 2007). While
16 these analyses give accurate predictions of how an implant will perform in a
17 representative case, they may not give good predictions of how an implant will
18 perform when released into a population because a medical device may perform
19 superbly in an average individual but will perform poorly in individuals whose
20 anatomy or pathology differ from average. The variable performance in a
21 population has been shown by, for example, the Swedish hip register where the
22 probability of a Müller hip prostheses lasting for 10 years is $81.7\% \pm 4.1\%$ (Malchau
23 et al., 1993) whereas for a Lubinus it is $96.3\% \pm 0.3\%$ (Kärrholm et al., 2007).
24 Awareness of the need to account for such differences in the range of performance
25 of different implants has led to a new wave of modelling approaches that attempt

1 to include aspects of population variability when simulating implant behaviour,
2 e.g. Laz et al., 2006; Viceconti et al., 2006; Knight et al., 2007; Dopico-Gonzalez
3 et al., 2009.

4 There are several factors that may cause variation in the outcome; these
5 may be classified as either environmental factors or genetic factors. Environment
6 factors include:

- 7 • surgical variation in implant positioning, as some implant designs may be
8 more sensitive to being inserted in non-optimal positions than others,
- 9 • loading, as each patient will subject the device to different loads
10 (Bergmann et al., 2001; Morlock et al., 2001; Heller et al., 2001)., and
- 11 • bone geometry, as no bones are identical (Noble et al., 1988; Fitzpatrick et
12 al., 2008) and implants may be sensitive to bone size and shape.

13 The genetic differences between patients that are particularly relevant to the
14 performance of a load-bearing implant include genetic variation in tissue
15 mechanoresponsiveness. As Frost (1987) speculated, each individual's bone tissue
16 has a somewhat different response to mechanical stress – and this
17 mechanosensitivity will also vary with age; some patients' bone tissue will be
18 indifferent to the change in stress whereas other bone tissue will be
19 mechanosensitive to a considerable degree leading to different amounts of bone
20 resorption around the implant, or different patterns of bone ingrowth. Many
21 follow-up studies have shown this; recently for example Panisello et al (2009)
22 showed that an anatomic non-cemented stem had bone loss which ranged from 12%
23 to 27% after 1 post-operative year.

1 In this paper we test the hypothesis that, if two devices are to be compared
2 an analysis based on an idealised or average patient will lead to different
3 conclusions than one that models the variability inherent in human populations.
4 To test this hypothesis a finite element model of an intramedullary implant is
5 used, with variability included in bone geometry and mechanosensitivity of the
6 bone tissue. An intramedullary implant is chosen as intramedullary fixation is
7 frequently used for many orthopaedic implants (Prendergast, 2001); furthermore,
8 Huiskes et al. (1987) used an axi-symmetric finite element model of an
9 intramedullary implant in the first computational studies of peri-prosthetic bone
10 remodelling. Later Prendergast and Taylor (1992) simulated remodelling around an
11 intramedullary implant using damage-adaptive remodelling. Because Young's
12 modulus is critical to the success of implant fixation (Weinans et al., 1992;
13 Scannell and Prendergast, 2009), it is varied in this study. If the hypothesis is
14 corroborated - for even this simplified intramedullary geometry - then this has
15 implications for how computational simulation of medical device performance is
16 conducted in the future.

17

18 **2 Methods**

19 The simplified intramedullary implant consisted of a hollow tube of homogeneous
20 cortical bone containing a tapered straight stem (Fig. 1). A force was applied to
21 the stem at nodes at the centre of its top surface while all nodes at the distal end
22 of the bone were restrained from movement. Total applied force to the stem was
23 calculated by estimating the equivalent force on the bone annulus to produce a
24 pressure that could induce an axial strain of $1,500 \mu\epsilon$ in the bone tube. This strain

1 magnitude was chosen as representative of a maximum strain in a long bone
2 diaphysis under normal conditions (Fritton and Rubin, 2001). Debonded contact
3 was assumed between the stem and bone with a friction coefficient of 0.3. A
4 region of elements near the restraints was excluded from the bone adaptation
5 simulation due to unphysiological strains arising from the restraints in this region.

6 The bone remodelling algorithm used in this study was presented in Mulvihill
7 and Prendergast (2008). Briefly, the algorithm follows the proposal of Frost (1983,
8 1987, 1990) that bone mechanoresponsiveness is categorised into four ‘windows’: a
9 disuse window where strain is below a minimum effective strain, denoted here as
10 ϵ_{\min} , an adapted window where no net change occurs between ϵ_{\min} and ϵ_{\max} , a
11 window where modelling occurs to create new bone mass on surfaces above ϵ_{\max} ,
12 and a pathologic region where matrix damage causes bone loss – in our
13 remodelling algorithm we denote this occurring above ω_{crit} . (In this study $\omega_{\text{crit}} =$
14 4.67×10^{-5} calculated assuming critical damage corresponds to the damage
15 occurring during one cycle of 4,000 $\mu\epsilon$. It is calculated based on a linear damage
16 rule (i.e. $\omega = N/N_f$ where N = number of cycles and N_f = cycles to failure at a given
17 stress) and an empirical equation for cycles to failure proposed by Carter et al.
18 (1976) is used, i.e., $\log N_f = H \log \sigma + J\theta + K\rho + M$ where σ , θ , ρ are stress (MPa),
19 temperature ($^{\circ}\text{C}$), and density (g/cm^3) respectively and $H = -7.789$, $J = -0.0206$, $K =$
20 -2.364 , $M = 15.47$ are empirical constants. Density is assumed to be 1.65 g/cm and
21 is used to calculate stress based on the density-modulus relationship noted below.
22 Temperature is assumed to be 37 $^{\circ}\text{C}$.)

23 During resorptive activity osteoclasts are assumed to resorb bone causing a
24 local rate of apparent density reduction of $-C \text{ g}/\text{cm}^3$ per day while during
25 formation osteoblast deposition is assumed to be a fraction, n , of osteoclast

1 resorption, giving a local rate of apparent density increase of nC g/cm³ per day;
 2 the resorption rate C was calculated based on an assumption that a BMU is capable
 3 of resorbing 1.4 $\mu\text{m}/\text{day}$ (Eriksen et al., 1984a) and that the ratio of formation to
 4 resorption is $n=0.31$ (Eriksen et al., 1984b). The following algorithm describes the
 5 four remodelling states:

If $\omega < \omega_{\text{crit}}$ then	
If $\varepsilon < \varepsilon_{\text{min}}$: $\dot{\rho} = -C$	Strain-based resorption (disuse)
Else if $\varepsilon > \varepsilon_{\text{max}}$: $\dot{\rho} = nC$	Strain-based formation (overuse)
Else: $\dot{\rho} = 0$	Remodelling equilibrium (stasis)
Else $\dot{\rho} = -C$	Damage-induced resorption (pathology)

6
 7 The algorithm for bone remodelling is illustrated in Fig. 2. This algorithm is used
 8 with a finite element analysis to simulate changes in bone density over time due to
 9 stress-shielding arising from introduction of the intramedullary stem.

10 Proceeding as illustrated in Fig. 2, the simulation is initiated by calculating
 11 the strain field within the bone using a finite element analysis. Each bone element
 12 is checked for remodelling status, and its rate of change of density is calculated
 13 according to the algorithm above. Next the apparent density change is calculated
 14 using the time step and element status as $\Delta\rho = \dot{\rho}\Delta t$. Stiffness of the element is
 15 then adapted according to a relationship between apparent density and Young's
 16 modulus, E , proposed by Carter and Hayes (1977) and as used by Weinans et al
 17 (1992):

$$18 \quad E = 3790 \rho^3 \quad \text{Eq. 1}$$

1 Upon reloading, the change in bone Young's modulus causes a change in the
2 resistance to stem displacement, leading to a different final position under peak
3 load relative to the previous step, and a new strain distribution, which is used to
4 drive the bone adaptation algorithm and update the material properties for the
5 next time step. Iterative execution of the algorithm over a series of time steps
6 thus simulates adaptation of the bone. As the stiffness of the bone tissue changes,
7 the motion of the implant relative to the bone changes, which results in prosthesis
8 migration over time. The simulation is terminated when the migration exceeds 3
9 mm.

10 Variability was introduced into the simulations by varying bone size and
11 mechanosensitivity. First, a scaling transformation was used to warp the extra-
12 cortical surface of the bone so that every case in the trial would have a different
13 diameter bone reflecting the variability that exists in the human population. A
14 uniform distribution for bone diameter was assumed in the population, and a
15 random number was generated within a range of 20 mm to 25 mm for the bone
16 diameter, taken from Noble et al (1988). Secondly, the strain-based resorption
17 (ϵ_{\min}) and formation (ϵ_{\max}) thresholds were also randomly generated in order to
18 represent variable mechanosensitivity, again assuming a uniform distribution, with
19 a range of $1,000 \pm 500 \mu\epsilon$ for ϵ_{\min} and $2,000 \pm 500 \mu\epsilon$ for ϵ_{\max} . Therefore the 'width'
20 of the zone of equilibrium strains in the reference case is $1,000 \mu\epsilon$, with variability
21 in the strain-based resorption (ϵ_{\min}) and formation (ϵ_{\max}) thresholds set, following
22 Frost (2003) as $\pm 500 \mu\epsilon$. Therefore the reference case representing idealized or
23 'average' bone has the following variables: bone external diameter = 22.5 mm, ϵ_{\min}
24 = $1,000 \mu\epsilon$, and $\epsilon_{\max} = 2,000 \mu\epsilon$.

1 In order to test the concept of a clinical trial for two intramedullary stems,
2 two sets of simulations were performed: one for a low stiffness implant (Young's
3 modulus = 20 GPa representing a lower bound for the Young's modulus of implant
4 materials; see Katti, 2004) and one for a stiff implant (Young's modulus = 200 GPa
5 representing steel). The simulated clinical trial consisted of 100 simulations per
6 implant, i.e. 200 simulations in total.

7

8 3 Results

9 For the reference ideal case, the change in bone strain during the simulation takes
10 on a different pattern depending on implant material. Among the differences are:

11 a) For the stiff implant a large region of strain-induced resorption occurs due
12 to a greater degree of immediate post-operative bulk bone stress reduction
13 whereas for the low stiffness implant damage-induced interfacial resorption
14 occurs in a small proximal region due to proximal interfacial damage, refer
15 to Fig. 3, time = 0 weeks, for evidence of this.

16 b) As the simulations progressed, interfacial damage-induced resorption
17 appeared around both stems but differed in spatial distribution; in the low
18 stiffness stem it progressed from proximal to distal whereas in the high
19 stiffness stem it initiated distally and progressed proximally. Refer to Fig. 3,
20 time = 10 weeks and time = 20 weeks.

21 c) Initially damaging of the *proximal* bone/implant interface occurs for the low
22 stiffness stem causes strain-induced proximal bone loss to occur whereas for
23 the high stiffness stem initial damaging of the *distal* bone/implant interface

1 interface occurs disconnecting the implant from the distal bone and placing
2 further load on the proximal bone thereby halting resorption, see Fig. 3,
3 time = 30 weeks. In other words complete opposite consequences of
4 interfacial damage-induced resorption occur vis-à-vis bulk bone remodelling
5 for high stiffness compared to low stiffness stems.

6 These aspects of the effect of materials selection on peri-prosthetic bone
7 adaptations has not been observed previously either because the remodelling
8 algorithms were simpler (Huiskes et al, 1987) or because the more complex
9 anatomical geometries mask the general nature of the biomechanics of
10 bone/implant systems (Scannell and Prendergast, 2009).

11 Referring to Fig. 4, quantitative analysis of the damage accumulation and
12 associated density changes in the bone tissue shows proximal (GZ1) damage is
13 initially greatest with the low stiffness stem but the damage obtained with the
14 high stiffness stem eventually exceeds it (Fig. 4a). On the other hand, the low
15 stiffness stem always induces a higher damage at the interface (Fig. 4a). Density
16 changes in the bone due to both strain and damage are shown in Fig 4b.

17 Reductions in bone density cause increased migration of the implant under a
18 cyclic load. In the reference case the mechanism causes a notable difference in
19 the migration rate of the two implants, with the stiffer 200 GPa implant migrating
20 more rapidly and thus failing more rapidly, than the low stiffness 20 GPa implant
21 (Fig. 5).

22 However, when the simulation is run on the whole population very
23 significant variation can be seen (Fig. 6) showing that the outcome is very variable
24 in a population. Analysis of time-to-failure data shows that there is no statistical

1 difference in the performance of the two implants in the population, despite the
2 differences in the performance of the reference case (Table 1).

3

4 **4 Discussion**

5 This study set out to test the hypothesis that an analysis based on a method for
6 predicting the performance in a population will lead to different conclusions than
7 an analysis based on an idealised average patient. Using an intramedullary implant
8 as an example, we found that the differences reported in an average idealised
9 case are not found in an analysis that simulates the behaviour of the implant when
10 used in a population. Deterministic analyses predicted that an intramedullary
11 implant made of low stiffness material would migrate less than a high stiffness
12 implant and should therefore have greater longevity; however our results show
13 that if the variability in a population is modelled this result no longer holds -the
14 data shows no statistical difference when variability of the kind that occurs in a
15 population was included. Therefore the factors causing a variable outcome in a
16 population are such that there is a significant overlap in the performance of two
17 designs of intramedullary-fixated implants is corroborated.

18 The limitations of this study are that the analysis pertains only to a
19 simplified intramedullary implant. A real anatomic bone shape and implant design
20 could have been used where, we might expect, the variability would be even
21 greater – in this respect it is more stringent to test the hypothesis in a simplified
22 geometry compared to a complex anatomical geometry where the variability would
23 be even greater. Similarly we could have varied other parameters such as the
24 loading whereas in these simulations the loading is proportional to bone cross-

1 sectional area so that each bone is assumed to have an identical pre-surgical
2 homeostatic strain level of $1500 \mu\epsilon$; again variation of loading or the homeostatic
3 strain assumption would be likely to further increase variability. A limitation of the
4 finite element analysis is that the bone properties used are isotropic and
5 homogeneous whereas it is known that bone stiffness is anisotropic and spatially
6 heterogeneous.

7 The bone remodelling algorithm used has been presented previously
8 (Mulvihill and Prendergast, 2008; Mulvihill and Prendergast, 2010) and is based on
9 the experimental work of (Lee et al., 2002) which associated microcracking with
10 bone adaptation and the earlier theoretical work of McNamara and Prendergast
11 (2007). The algorithm has been partly corroborated previously against simulations
12 in 3D around noncemented total hip replacements (Scannell and Prendergast,
13 2009). Finally in this study no consideration was given to the possible repair of the
14 interface when the resorbed tissue is replaced by soft tissue and then bone in a
15 process of osseointegration (Prendergast, 2007).

16 The results presented here have implications for the conduct of preclinical
17 testing using finite element modelling (Stolk et al., 2007). It suggests that
18 simulations of implants in population-averaged or “ideal” anatomies may lead to
19 conclusions that one implant is superior to another would not be borne out in a
20 clinical trial. Since computational power is now sufficient to do simulations of
21 clinical trials of the kind presented here then there is a case that these should be
22 included in pre-clinical testing platforms used in seeking regulatory approval for
23 devices. Such pre-clinical analyses could be aided by making available reference
24 libraries of models of skeletal and other relevant anatomical structures, perhaps
25 even different libraries for different ethnic groups reflecting differences in

1 anatomy. Results of this study also suggest the importance of mechanoregulation
2 parameters, which will also be variable in the population due to genetic
3 differences and age variability in patients (Frost, 1987; Khayyeri et al., 2011).

4 In this study we have simulated a clinical trial on a simplified intramedullary
5 implant. We have shown that, despite discernable differences in implants when
6 analyses are performed on standard cases, there is no statistically significant
7 difference when the implants are subjected to a simulated clinical trial.

8 A further aspect to be considered is that it is not the average performance
9 that is important, but rather the proclivity to perform below par in a percentage
10 of cases. Computational simulations of clinical trials have the potential to analyse
11 this aspect of the behaviour of an implant design

12 In conclusion this study has identified that it is possible to perform a
13 simulation of a clinical trial, and that such simulations have a value over and above
14 analyses performed in idealised population-averaged reference cases since
15 simulated clinical trials lead to different conclusions. It is proposed that these
16 kinds of simulations be carried out taking account of the differences in the
17 response of tissues to mechanical stress, as well as variations in anatomy.
18 Furthermore an advantage of this kind of work is that the results are, in principle,
19 validatable against the results of the clinical trial. If this proved to be true then it
20 would overcome one of the most often made criticisms of computer modelling in
21 implant analysis: the lack of falsifiability of the models.

22 **Acknowledgements**

- 1 The research reported in this paper has been funded by a Principal Investigator
- 2 grant to P. J. Prendergast funded by Science Foundation Ireland.

3

ACCEPTED MANUSCRIPT

1 **References**

2

3 Bergmann, G., Deuretzbacher, G., Heller, M., Graichen, F., Rohlmann, A., Strauss,
4 J., Duda, G.N., 2001. Hip contact forces and gait patterns from routine
5 activities. *J Biomech* 34, 859-71.

6 Carter, D.R., Hayes, W.C., 1977. The compressive behavior of bone as a two-phase
7 porous structure. *J Bone Joint Surg Am* 59, 954-62.

8 Carter, D.R., Hayes, W.C. and Schurman, D.J., 1976, Fatigue life of compact bone
9 II - effects of microstructure and density. *Journal of Biomechanics* 9, 211-
10 218.

11 Dopico-Gonzalez, C., New, A.M., Browne, M., 2009. Probabilistic analysis of an
12 uncemented total hip replacement. *Medical Engineering & Physics* 31, 470 -
13 476.

14 Eriksen, E.F., Gundersen, H.J., Melsen, F., Mosekilde, L., 1984a. Reconstruction of
15 the formative site in iliac trabecular bone in 20 normal individuals
16 employing a kinetic model for matrix and mineral apposition. *Metab Bone*
17 *Dis Relat Res* 5, 243-52.

18 Eriksen, E.F., Melsen, F., Mosekilde, L., 1984b. Reconstruction of the resorptive
19 site in iliac trabecular bone: a kinetic model for bone resorption in 20
20 normal individuals. *Metab Bone Dis Relat Res* 5, 235-42.

21 Fitzpatrick, C.K., FitzPatrick, D.P., Auger, D.D., 2008. Size and shape of the
22 resection surface geometry of the osteoarthritic knee in relation to total

- 1 knee replacement design. Proceedings of the Institution of Mechanical
2 Engineers, Part H: Journal of Engineering in Medicine 222, 923-932.
- 3 Fritton, S.P., Rubin C.T., 2001, In vivo measurements of bone deformations using
4 strain gauges. In Bone Mechanics Handbook (Editor: S.C. Cowin), Chapter 8
- 5 Frost, H.M., 1983. A determinant of bone architecture. The minimum effective
6 strain. Clin. Orthop. Relat. Res 286-292.
- 7 Frost, H.M., 1987, Bone “mass” and the “mechanostat”: a proposal. Anatomical
8 Record 219, 1-9
- 9 Frost, H.M., 1990. Skeletal structural adaptations to mechanical usage (SATMU): 1.
10 Redefining Wolff's law: the bone modeling problem. Anat Rec 226, 403-13.
- 11 Frost, H.M., 2003. Bone's mechanostat: a 2003 update. Anat Rec A Discov Mol Cell
12 Evol Biol 275, 1081-1101.
- 13 Helgason, B., Perilli, E., Schileo, E., Taddei, F., Brynjólfsson, S., Viceconti, M.,
14 2008. Mathematical relationships between bone density and mechanical
15 properties: a literature review. Clin Biomech 23, 135-146.
- 16 Heller, M.O., Bergmann, G., Deuretzbacher, G., Dürselen, L., Pohl, M., Claes, L.,
17 Haas, N.P., Duda, G.N., 2001. Musculo-skeletal loading conditions at the hip
18 during walking and stair climbing. Journal of Biomechanics 34, 883-893.
- 19 Heller, M.O., Bergmann, G., Kassi, J., Claes, L., Haas, N.P., Duda, G.N., 2005.
20 Determination of muscle loading at the hip joint for use in pre-clinical
21 testing. J Biomech 38, 1155-1163.

- 1 Huiskes, R., Chao, E.Y., 1983. A survey of finite element analysis in orthopedic
2 biomechanics: The first decade. *Journal of Biomechanics* 16, 385-409.
- 3 Huiskes, R., Weinans, H., Grootenboer, H.J., Dalstra, M., Fudala, B., Slooff, T.J.,
4 1987. Adaptive bone-remodeling theory applied to prosthetic-design
5 analysis. *J Biomech* 20, 1135-50.
- 6 Kärrholm, J., Garellick, G., Rogmark, C., Herberts, P., 2007. Swedish Hip
7 Arthroplasty Register: Annual Report 2007. *Acta Orthop Scand*.
- 8 Katti, K.S., 2004, Biomaterials in total joint replacement. *Colloids and Surfaces B:*
9 *Biointerfaces* 39, 133-142
- 10 Khayyeri, H., Checa, S., Tagil, M., Aspenberg, P., and PJ Prendergast, P.J., 2011,
11 Variability observed in mechano-regulated in vivo tissue differentiation can
12 be explained by variation in cell mechanosensitivity. *Journal of*
13 *Biomechanics* 44, 1051-1058 , 2011
- 14 Knight, L.A., Pal, S., Coleman, J.C., Bronson, F., Haider, H., Levine, D.L., Taylor,
15 M., Rullkoetter, P.J., 2007. Comparison of long-term numerical and
16 experimental total knee replacement wear during simulated gait loading. *J*
17 *Biomech* 40, 1550-8.
- 18 Laz, P.J., Pal, S., Halloran, J.P., Petrella, A.J., Rullkoetter, P.J., 2006.
19 Probabilistic finite element prediction of knee wear simulator mechanics.
20 *Journal of Biomechanics* 39, 2303 - 2310.
- 21 Lee, T.C., Staines, A., Taylor, D., 2002. Bone adaptation to load: microdamage as
22 a stimulus for bone remodelling. *J. Anat* 201, 437-446.

- 1 Lennon, A.B., Britton, J.R., MacNiocaill, R.F., Byrne, D.P., Kenny, P.J.,
2 Prendergast, P.J., 2007. Predicting revision risk for aseptic loosening of
3 femoral components in total hip arthroplasty in individual patients--a finite
4 element study. *Journal of Orthopaedic Research* 25, 779-88.
- 5 Malchau, H., Herberts, P., Ahnfelt, L., 1993. Prognosis of total hip replacement in
6 Sweden: Follow-up of 92,675 operations performed 1978-1990. *Acta*
7 *Orthopaedica* 64, 497-506.
- 8 McNamara, L.M., Prendergast, P.J., 2007, Bone remodelling algorithms
9 incorporating both strain and microdamage stimuli, *Journal of Biomechanics*
10 40, 1381-1391, 2007
- 11 Morlock, M., Schneider, E., Bluhm, A., Vollmer, M., Bergmann, G., Müller, V.,
12 Honl, M., 2001. Duration and frequency of every day activities in total hip
13 patients. *Journal of Biomechanics* 34, 873 - 881.
- 14 Mulvihill, B.M., Prendergast, P.J., 2008. An algorithm for bone
15 mechanoresponsiveness: implementation to study the effect of patient-
16 specific cell mechanosensitivity on trabecular bone loss. *Comput Methods*
17 *Biomech Biomed Engin* 11, 443-451.
- 18 Mulvihill, B.M., Prendergast P.J., 2010, Mechanobiological regulation of the
19 remodelling cycle in trabecular bone and possible biomechanical pathways
20 for osteoporosis *Clinical Biomechanics* 25: 491-498
- 21 Noble, P., Alexander, J., Lindahl, L., Yew, D.T., Granberry, W., Tullos, H., 1988.
22 The anatomic basis of femoral component design. *Clinical Orthopaedics and*
23 *Related Research* 148-165.

- 1 Panisello, J.J., Herrero, L., Canales, V., Herrera, A., Martínez, A.A., Mateo, J.,
2 2009. Long-term remodeling in proximal femur around a hydroxyapatite-
3 coated anatomic stem: ten years densitometric follow-up. *Journal of*
4 *Arthroplasty* 24, 56-64.
- 5 Prendergast, P.J., 1997. Finite element models in tissue mechanics and
6 orthopaedic implant design. *Clinical Biomechanics* 12, 343-368.
- 7 Prendergast, P.J., 2001, Bone Prostheses and Implants. In *Bone Mechanics*
8 *Handbook* (Editor: S.C. Cowin), Chapter 35, pp. 35.1-35.39
- 9 Prendergast, P.J. 2007, Combining mechanoregulation algorithms for bone
10 remodelling and tissue differentiation. In *Bioengineering Modelling and*
11 *Computer Simulation* (Ed.: Y. González & M. Cerrolaza), International
12 Center for Numerical Methods in Engineering: Barcelona, pp. 238-248, 2007
- 13 Prendergast, P.J., Taylor, D., 1992. Design of intramedullary prostheses to prevent
14 bone loss: predictions based on damage-stimulated remodelling. *J Biomed*
15 *Eng* 14, 499-506.
- 16 Scannell, P.T., Prendergast, P.J., 2009. Cortical and interfacial bone changes
17 around a non-cemented hip implant: simulations using a combined
18 strain/damage remodelling algorithm. *Medical Engineering and Physics* 31,
19 477-488.
- 20 Stolk, J., Janssen, D., Huiskes, R., Verdonschot, N., 2007. Finite element-based
21 preclinical testing of cemented total hip implants. *Clin Orthop Relat Res*
22 456, 138-47.

- 1 Taylor, M., Barrett, D.S., 2003. Explicit Finite Element Simulation of Eccentric
2 Loading in Total Knee Replacement. *Clinical Orthopaedics and Related*
3 *Research* 414, 162-171.
- 4 Verdonchot, N., Huiskes, R., 1997. The effects of cement-stem debonding in THA
5 on the long-term failure probability of cement. *Journal of Biomechanics* 30,
6 795-802.
- 7 Viceconti, M., Brusi, G., Pancanti, A., Cristofolini, L., 2006. Primary stability of an
8 anatomical cementless hip stem: A statistical analysis. *Journal of*
9 *Biomechanics* 39, 1169 - 1179.
- 10 Weinans, H., Huiskes, R., Grootenboer, H.J., 1992. Effects of material properties
11 of femoral hip components on bone remodeling. *J Orthop Res* 10, 845-53.

1 List of Figures

2 Figure 1: A 3D finite element mesh of an intramedullary implant of the reference
3 dimension of 22.5 mm external bone diameter. Note that the loading applied to
4 the implant is that which would give a 1,500 $\mu\epsilon$ in the longitudinal direction were
5 it applied directly to the bone surface.

6 Figure 2: An illustration of the bone remodelling algorithm. A finite element model
7 is used to compute the stress and strain in the bone tissue. If damage (denoted ω)
8 is above a critical value then the tissue is pathologically injured and it resorbs,
9 otherwise strain-adaptive remodelling occurs as follows: if strain (denoted ϵ) is
10 above a threshold then addition of bone tissue occurs otherwise if it is below a
11 threshold then resorption occurs, otherwise it is in homeostasis and neither
12 resorption or deposition occurs. When the changes computed are very low the
13 structure is converged and the algorithm 'exits'.

14 Figure 3: Contour plots of strain and damage activity at different time points
15 during the simulation for the reference ideal 'average' cases for each stem. Note
16 that the reference case is with a bone external diameter of 22.5 mm, $\epsilon_{\min} = 1000$
17 $\mu\epsilon$ and $\epsilon_{\max} = 2000 \mu\epsilon$.

18 Figure 4: A detailed analysis of (a) the damage accumulation and (b) associated
19 density changes in the bone tissue. Note that GZ stands for Gruen Zone, i.e. a
20 region of the bone surrounding the implant.

21 Figure 5: In the reference case there is a difference in the subsidence rate of the
22 two implants, with the 20 GPa implant migrating more rapidly and this failing more
23 rapidly, than the 200 GPa implant.

24 Figure 6: When all analyses are run (100 per implant, therefore 200 in total) very
25 significant variation in subsidence is predicted. Statistical analysis shows that
26 there is no statistical difference between the performance of the implants (refer
27 to Table 1).

28

1 **List of Tables**

- 2 **Table 1:** Analysis of time-to-failure data shows that there is no statistical
3 difference in the performance of the two implants in the population, despite the
4 apparent differences in the performance of the reference models.

ACCEPTED MANUSCRIPT

1 **Table 1:** Analysis of time-to-failure data shows that there is no statistical
 2 difference in the performance of the two implants in the population, despite the
 3 apparent differences in the performance of the reference models.

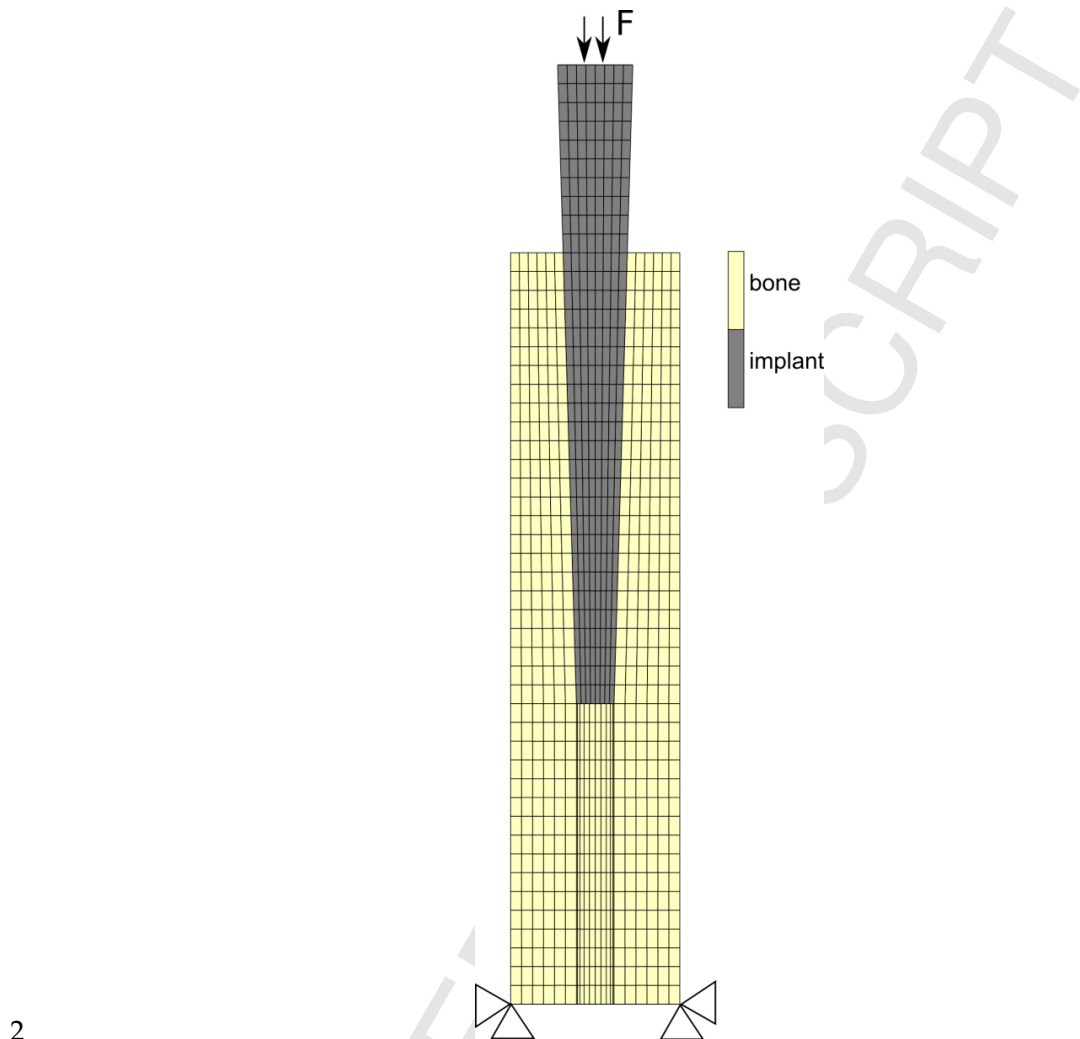
	E=20 GPa	E=200 GPa
Mean	45.58	45.91
Median	44.75	45.83
Standard Deviation	35	44
Sample Variance	8.14	7.62
Kurtosis	66.33	58.10
Skewness	-0.85	-0.64
Range	30	30
Minimum	34	32
Maximum	64	62
Confidence Interval (95.0%)	1.51	1.62
<i>p (t-test)</i>		0.77

4

5

6

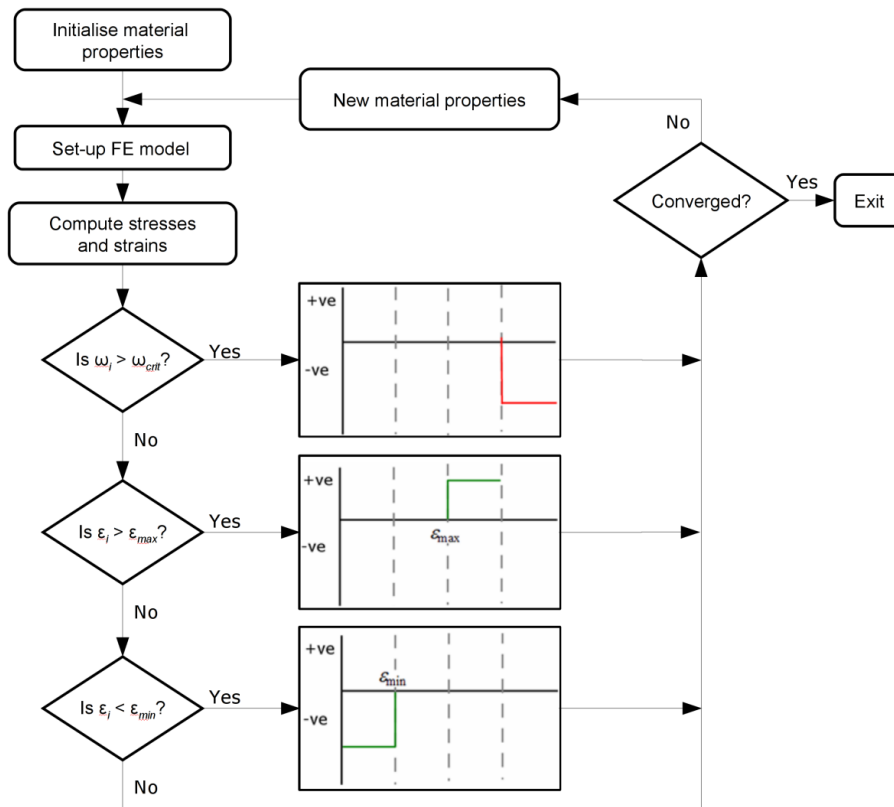
1



5 **Figure 1:** A 3D finite element mesh of an intramedullary implant of the reference
6 dimension of 22.5 mm external bone diameter. The loading applied to the implant
7 is that which would give a $1,500 \mu\epsilon$ in the longitudinal direction were it applied
8 directly to the bone surface.

1

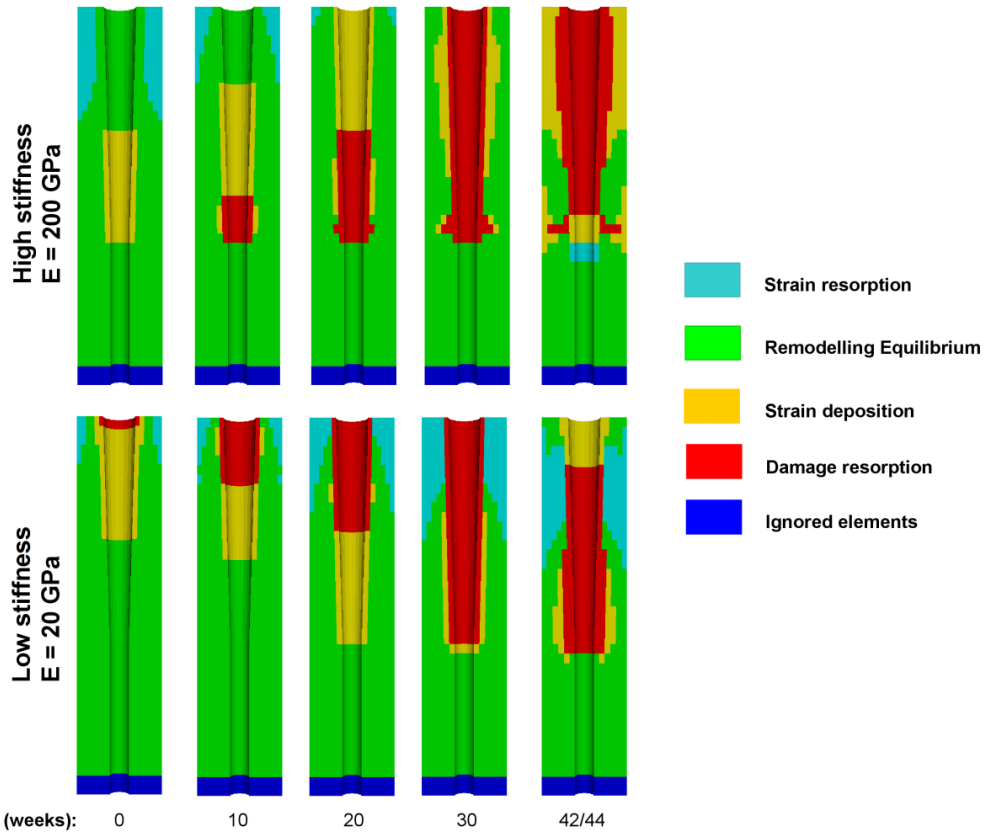
2



3

4 **Figure 2:** An illustration of the bone remodelling algorithm. A finite element
 5 model is used to compute the stress and strain in the bone tissue. If damage
 6 (denoted ω) is above a critical value then the tissue is pathologically injured by
 7 microcracking and it resorbs, otherwise strain-adaptive remodelling occurs as
 8 follows: if strain (denoted ϵ) is above a threshold then addition of bone tissue
 9 occurs otherwise if it is below a threshold then resorption occurs, otherwise it is in
 10 homeostasis and neither resorption or deposition occurs. When the changes
 11 computed are very low the structure is converged and the algorithm 'exits'.

1

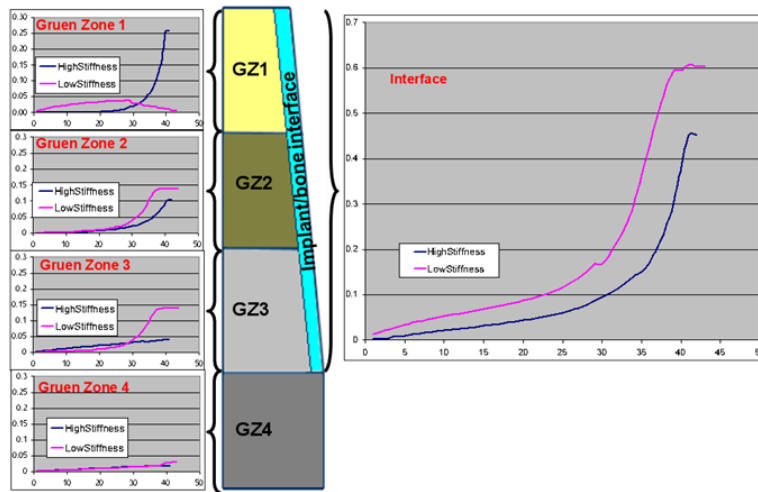


2

3

4 **Figure 3:** Contour plots of strain and damage activity at different time points
 5 during the simulation for the reference ideal ‘average’ cases for each stem. Note
 6 that the reference case is with a bone external diameter of 22.5 mm, $\epsilon_{\min} = 1000$
 7 $\mu\epsilon$ and $\epsilon_{\max} = 2000 \mu\epsilon$.

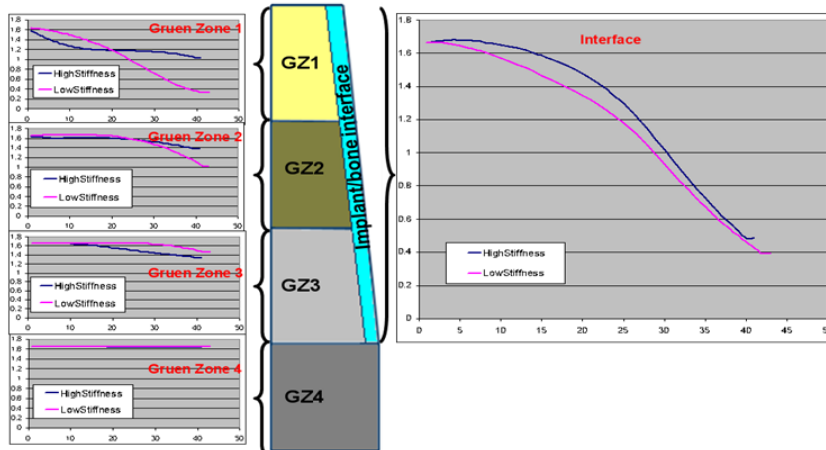
1

Damage results for reference models: 22.5 mm, 0.001, 0.002

2

3

(a)

Density results for reference models: 22.5 mm, 0.001, 0.002

4

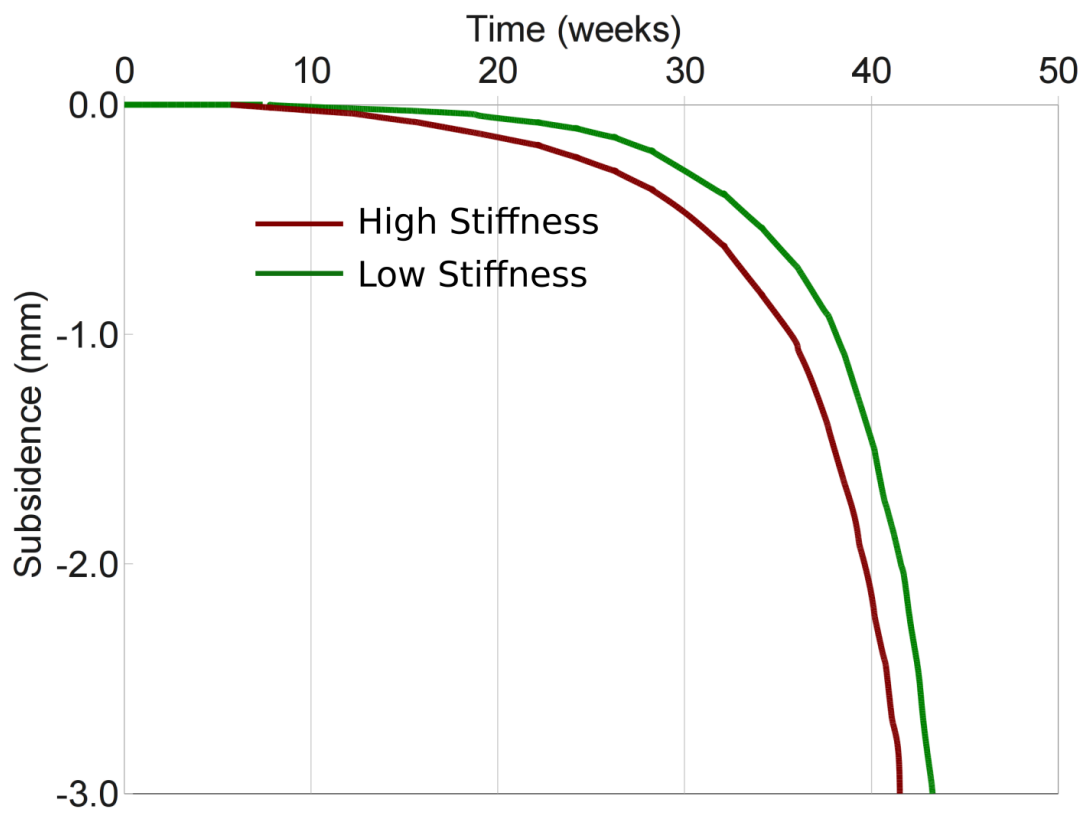
5

6

(b)

7 **Figure 4:** A detailed analysis of (a) the damage accumulation and (b) associated
 8 density changes in the bone tissue. Note that GZ stands for Gruen Zone, i.e. a
 9 region of the bone surrounding the implant.

1

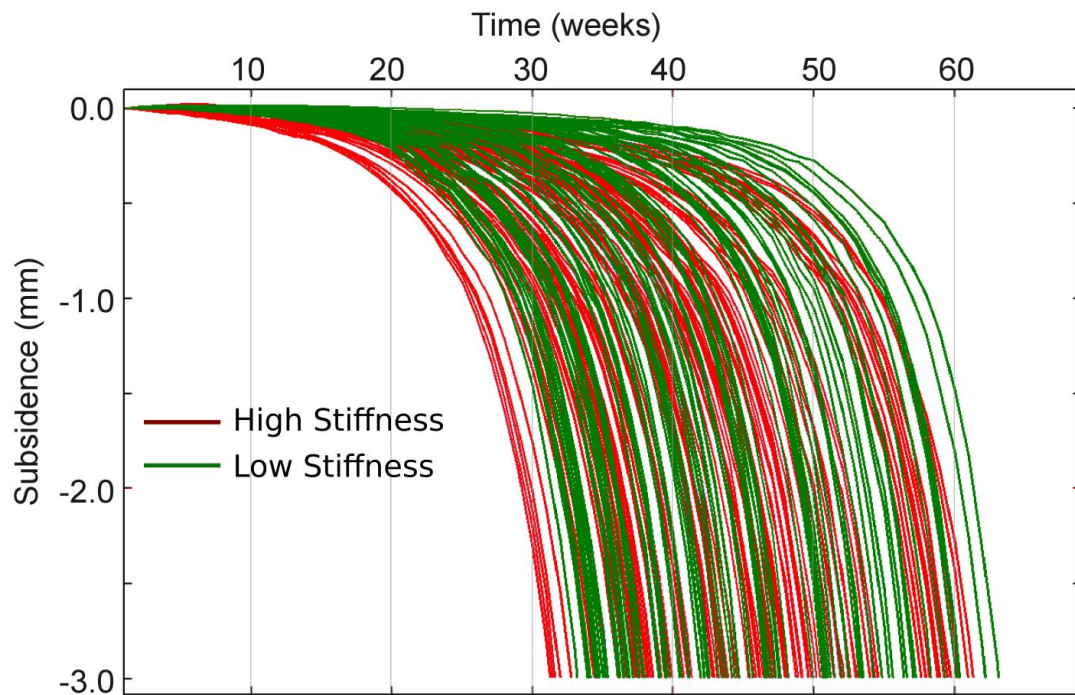


2

3 **Figure 5:** In the reference case there is a difference in the subsidence rate of the
4 two implants, with the 20 GPa implant migrating more rapidly and this failing more
5 rapidly, than the 200 GPa implant.

6

1



2

3

4 **Figure 6:** When all analyses are run (100 per implant, therefore 200 in total) very
5 significant variation is in subsidence is predicted. Statistical analysis shows that
6 there is no statistical difference between the performance of the implants (refer
7 to Table 1).

8